

Numerical Calculation of Sound Radiation from Structures Containing a Porous Layer Sandwiched by Double Walls with Krylov Type Acoustic Black Hole

Takao Yamaguchi^{1,a,*}, Chihiro Kamio^{1,b}, Tomoki Tamura^{2,c}
and Yuta Hisamura^{2,d}

¹Gunma University, 1-5-1 Tenjin-cho, Kiryu, Gunma, 376-8515 Japan

²Graduate School of Gunma University, 1-5-1 Tenjin-cho, Kiryu, Gunma, 376-8515 Japan

*Corresponding author

^a<yamagme3@gunma-u.ac.jp >, ^b<chihiro.kamio@gunma-u.ac.jp >

Keywords: acoustic black hole, sound radiation, finite element method, damping, porous layer

Abstract. Noise reduction is an important technology to obtain comfort environment. In this report, we perform numerical computation of sound radiation from a structure containing a porous layer sandwiched by double walls. The cover plate in the double walls has a Krylov type acoustic black hole. All edges in the cover plate where the black hole exists, are set as free boundaries. Viscoelastic damping material is laminated on the top of the black hole. Numerical analysis is carried out to investigate sound radiation from this structure using FEM and MSKE method which is proposed by Yamaguchi et al.

1. Introduction

With Double walls having a porous layer are well-known effective approach to decrease noise due to sound radiation from vibrations in panels. Many researchers have been studied about these structures. In this paper, we call two plates in the double walls as base plate and cover plate.

On the other hand, some researchers have been investigated acoustic black holes as an effective approach of vibration reduction [18]. This concept was proposed by Mironov [1]. Mironov studied vibration propagations of bending waves in a flat plate having an edge where the thickness of the plates decreasing to the edge as a quadratic function x^2 of the distance x from the boundary. Due to the black hole, it is difficult that the bending waves reflect at the edge. Mironov called this structure as acoustic black hole. But, to obtain sufficient vibration reduction effects, it is necessary that the length of the edge is enough long. At the edge, the thickness is too thin to compensate the strength of the structures. To improve this, Krylov proposed to modify the Mironov's acoustic black hole [2]-[5] by cutting off the edge practically as finite length. Further, Krylov added a thin viscoelastic damping layer on the edge. According to Oberst theory [6], vibration damping effects of a straight metal beam covered with a viscoelastic layer are proportional to (thickness of the damping layer/ thickness of the metal beam)². Thus, high efficient damping effects appear when a viscoelastic damping layer is covered on the edge in the black hole because of thin thickness around the black holes.

In this paper, we investigate effects of adoption of the acoustic black hole to the cover plate in the double walls on sound radiation. To evaluate effects of the acoustic black holes, we carry out vibration damping analysis and sound radiation analysis after vibration response analysis using finite element method for structures having acoustic black holes in the double walls under dynamic loads. We computed modal loss factors, vibration responses. By using these results, we calculated acoustic radiation power from the cover plate.

2. Calculation Model

To investigate effects of the acoustic black holes on reduction of sound radiation in the double walls having a porous layer, we use calculation models as shown in Figs. 1 and 2.

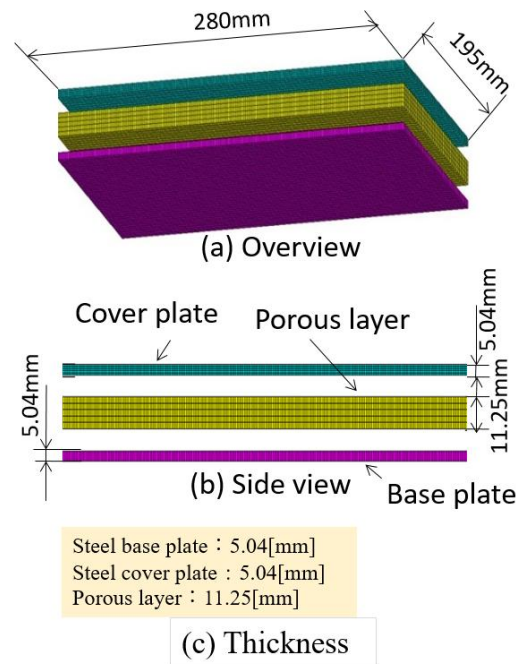


Fig. 1. FEM model including cover plate without acoustic black hole (Model 1).

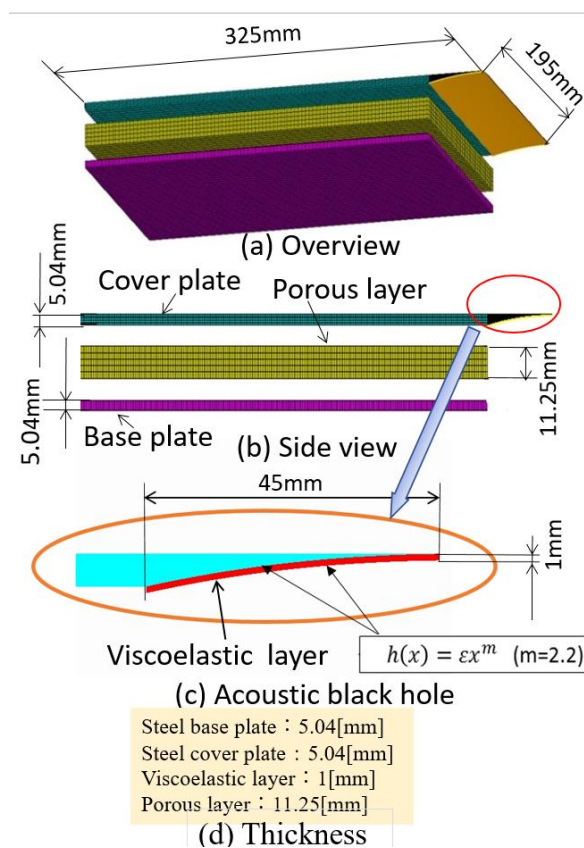


Fig. 2. FEM model including cover plate with acoustic black hole having viscoelastic layer (Model 2).

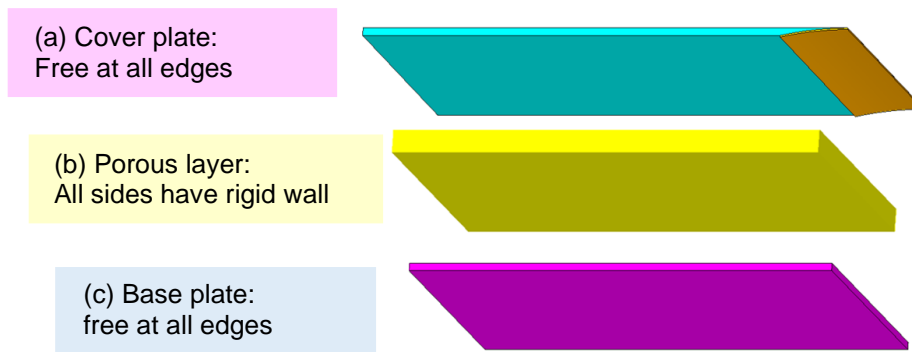


Fig. 3. Boundary conditions.

As shown in Fig.1, the double walls have a steel base plate and a steel cover plate denoted as “model 1”. A porous layer is sandwiched between the base plate and the cover plate. Thickness of the base plate is 5.04mm, and thickness of the cover plate is also 5.04mm. the thickness of the porous layer is 11.25mm. As shown in Fig.2, the Krylov’ type acoustic black hole is added to one of edges in the cover plate. Around the edge of the cover plate, the thickness $h(x)$ of the plate decreases according to the function $h(x)= \varepsilon x^{2.2}$ for the Krylov’s acoustic black hole . Where, x is the distance from the edge. A viscoelastic damping layer is covered on the regions around the black hole. Thickness of the viscoelastic damping layer is 1.0mm. Geometry of the cover plate is same as the plate in the Krylov’s experiment [5]. The boundary conditions are denoted in Fig.3.

Around the cover plate, all edges are set as free. All edges around the base plate are also set as free. For the porous layer, all sides have rigid wall. At the boundaries between the solid bodies (i.e. the base plate and the cover plate) and the porous layer, the normal components of the displacements to the boundaries are continuous. On the other hand, the tangential components of the displacements along the boundaries are independent.

As illustrated in Fig.4, the excitation point is set at 5 mm away in z-direction from the center of the base plate. At this point, white noise is given as input wave.

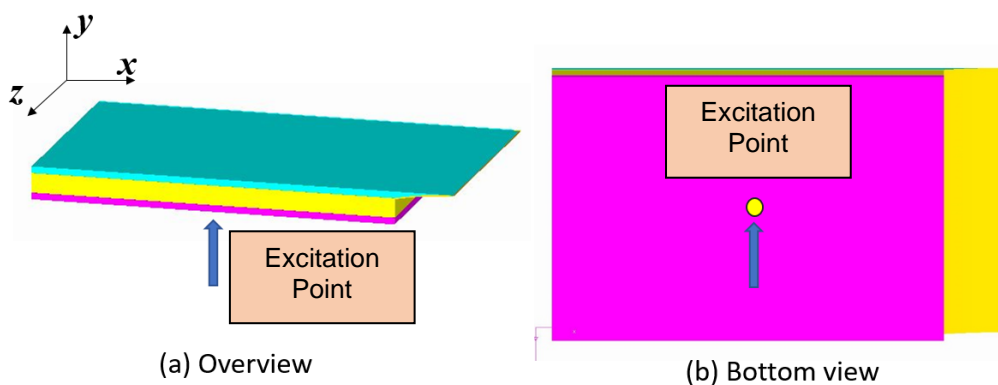


Fig. 4. Excitation point.

3. Calculation Procedure

To consider the mixed problem containing arbitrary shapes and arbitrary boundary conditions, the porous body, the solid bodies are modeled using finite elements for the double walls having the porous layer and the acoustic black hole. To evaluate modal loss factors of the coupled mixed structures, we use MSKE method [7]-[11]. Further, we compute vibration responses and sound radiation.

3.1 Discrete Equations in Porous Layer

For the internal air in the porous layer, we use a finite element model as shown in this section. Considering periodic oscillation and infinitesimal amplitude, the equations of motion can be written for inviscid compressive perfect fluid as follows.

$$-\text{grad } p = -\rho_e \omega^2 \{u_f\} \quad (1)$$

The continuity equation is shown as:

$$p = -E_e \text{div}\{u_f\} \quad (2)$$

$\{u_f\}$ is the particle displacements vector. p denotes sound pressure. ρ represents the effective density of the internal air. E represents the modulus of volume elasticity of the internal air. ω is the angular frequency. Here, the particle displacements $\{u_f\}$ are chosen as unknowns [7]-[11] by eliminating the sound pressure p in Eqns. (1) and (2). The displacement is chosen as the common unknown variable for the double walls structure with acoustic black hole.

We approximate the relation between $\{u_f\}$ and particle displacement vectors $\{u_{fe}\}$ at nodal points in the element as

$$\{u_f\} = [N_f]^T \{u_{fe}\} \quad (3)$$

Where, $[N_f]^T$ represents a matrix comprised of proper shape functions.

From Eqs (1), (2) and (3), the strain energy, kinetic energy, and external work can be determined. After applying the Minimum Energy Principle, the following equations are obtained.

$$([K]_{fe} - \omega^2 [M]_{fe}) \{u_{fe}\} = \{f_{fe}\} \quad (4)$$

$$[K]_{fe} = E_e [\tilde{K}]_{fe} \quad (5)$$

$$[M]_{fe} = \rho_e [\tilde{M}]_{fe} \quad (6)$$

E_e and ρ_e show the volume elasticity and the effective density in the domain of the elements, respectively. $[K]_{fe}$ and $[M]_{fe}$ show the element stiffness matrix and the element mass matrix, respectively. $[\tilde{K}]_{fe}$, $[\tilde{M}]_{fe}$ show the matrix including the shape functions and their derivatives. $\{f_{fe}\}$ is the nodal force vector.

We utilize the following model having the complex effective density ρ_e^* and complex volume elasticity E_e^* , for damped sound fields inside porous materials [12],[7]-[11]:

$$\rho_e \Rightarrow \rho_e^* = \rho_{eR} + j\rho_{eI} \quad (7)$$

$$E_e \Rightarrow E_e^* = E_{eR} + jE_{eI} \quad (8)$$

Where, j is the imaginary unit. ρ_{eR} and ρ_{eI} are the real and imaginary parts of ρ_e^* , respectively. E_{eR} and E_{eI} show the real and imaginary parts of E_e^* , respectively. We verified that this model is suitable for fibrous materials in cars [7]-[10]. We assumed the elastic waves [13]-[15] through the resin fiber of the porous materials can be neglected.

Element mass matrix $[M]_{fe}$ can be written by substituting Eqn. (7) into Eqn. (6).

$$[M]_{fe} = [M_R]_{fe}(1 + j\chi_{fe}) \quad (9)$$

$$\chi_{fe} = \rho_{el}/\rho_{eR} \quad (10)$$

$[M_R]_{fe}$ is the real part of the element mass matrix $[M]_{fe}$. ρ_{el} is the imaginary part of the effective density. $\chi_{fe} = \rho_{el}/\rho_{eR}$ shows the damping effect originated from flow resistance.

Substituting Eqn.(8) into Eqn.(5), the following element stiffness matrix $[K]_{fe}$ is given.

$$[K]_{fe} = [K_R]_{fe}(1 + j\eta_{fe}) \quad (11)$$

$$\eta_{fe} = E_{el}/E_{eR} \quad (12)$$

In Eq. (11), $[K_R]_{fe}$ shows the real part of the element stiffness matrix $[K]_{fe}$. In Eq. (12), η_{fe} shows the damping effect due to hysteresis between pressure and volume strain in the porous materials.

Both the element mass matrix $[M_R]_{fe}$ and the element stiffness matrix $[K]_{fe}$ for internal gas in the porous materials have complex quantities.

The complex effective density is $\rho_{eR}=1.40\text{kg/m}^3$, $\chi_{fe}=-0.500$. And the complex volume elasticity is $E_{eR}=1.19 \times 10^5\text{N/m}^2$, $\eta_{fe} =0.100$. For the porous layer in the double-walled structures, the isoparametric hexagonal elements are used.

3.2 Equation for Vibration of Solid Bodies with Damping in the Double Walls

We used discretized equations shown in the following equations from Eqns. (13) to (15) for vibration of the cover plate and the base plate with the acoustic black hole. For the viscoelastic layer on the acoustic black hole, we use the same model. These models are considered as conventional linear finite element model with hysteresis damping.

$\{u_s\}$ shows the displacement vector for the solid bodies. Using the matrix comprised of shape functions $[N_s]^T$, the relation between the displacements $\{u_{se}\}$ at nodal points and the displacement vector $\{u_s\}$ in an element for the solid bodies are approximated as:

$$\{u_s\} = [N_s]^T \{u_{se}\} \quad (13)$$

Strain energy, kinetic energy, and external work are determined, and then, by applying the Lagrange equation, the following expressions are given.

$$([K]_{se} - \omega^2[M]_{se})\{u_{se}\} = \{f_{se}\} \quad (14)$$

$$[K]_{se} = [K_R]_{se}(1 + j\eta_{se}) \quad (15)$$

$[K]_{se}$ and $[M]_{se}$ represent the element stiffness matrix and element mass matrix, respectively. $\{f_{se}\}$ shows the nodal force vector in an element e for the solid bodies. The element stiffness matrix $[K_R]_{se}$ in Eqn.(15) has complex quantities in Eqn. (14). $[K_R]_{se}$ shows the real part of element stiffness matrix for the solid bodies. η_{se} shows the material loss factor related with element e .

For the viscoelastic materials and the elastic materials, the isoparametric hexahedral elements are mainly used with the non-conforming modes. For the viscoelastic damping material, the storage modulus of elasticity is $1.6 \times 10^9 \text{ N/m}^2$, the mass density is $1.9 \times 10^3 \text{ kg/m}^3$ and the material loss factor η_{se} is 0.5.

3.3 Discrete Equations for the Global System of the Double Walls with Acoustic Black Hole

All elements for the porous layer and the base plate and the cover plate in the double walls having the acoustic black hole are superposed by using equations from Eqns. (4) to (15). At boundaries between the porous layer and the solid bodies (i.e. the cover plate and the base plate), normal components of the displacements to the boundaries are continuous. Tangential components of the displacements along the boundaries are independent. From these conditions, the following equation is given.

$$([K]_a - \omega^2[M]_a)\{u_a\} = \{f_a\} \quad (16)$$

Where, $\{f_a\}$ shows the nodal force vector and $\{u_a\}$ shows the nodal displacement vector. $\{u_a\}$ is comprised of $\{u_{fe}\}$ and $\{u_{se}\}$. $[K]_a$ contains $[K]_{fe}$ and $[K]_{se}$, while $[M]_a$ includes $[M]_{fe}$ and $[M]_{se}$.

3.4 Equations for Modal Damping by Using MSKE Method [7]-[11]

By ignoring the external force vector from Eq. (16), we can obtain the following complex eigenvalue problem:

$$\sum_{e=1}^{e_{\max}} ([K_R]_e (1 + j\eta_e) - (\omega^{(i)})^2 (1 + j\eta_{\text{tot}}^{(i)}) [M_R]_e (1 + j\chi_e)) \{\phi^{(i)*}\} = \{0\} \quad (17)$$

Where, superscript (i) represents the i -th eigenmode. $(\omega^{(i)})^2$ shows the real part of complex eigenvalue. $\{\phi^{(i)*}\}$ shows the complex eigenvector and $\eta_{\text{tot}}^{(i)}$ represents the modal loss factor. $[K_R]_e$ shows the real part of element stiffness matrix. $[M_R]_e$ denotes the real part of element mass matrix.

Next, the following parameters β_{se} and β_{ke} are introduced:

$$\beta_{se} = \frac{|\eta_e|}{\eta_{\max}}, \quad \beta_{se} \leq 1, \quad \beta_{ke} = \frac{|\chi_e|}{\eta_{\max}}, \quad \beta_{ke} \leq 1 \quad (18)$$

η_{\max} shows the maximum value among the elements' material loss factors η_e and χ_e , ($e = 1, 2, 3, \dots, e_{\max}$). Under assumption of $\eta_{\max} \ll 1$, solutions of Eq. (17) can be expanded using a small parameter $\mu = j\eta_{\max}$ [16]:

$$\{\phi^{(i)*}\} = \{\phi^{(i)}\}_0 + \mu\{\phi^{(i)}\}_1 + \mu^2\{\phi^{(i)}\}_2 + \dots \quad (19)$$

$$(\omega^{(i)})^2 = (\omega_0^{(i)})^2 + \mu^2(\omega_2^{(i)})^2 + \mu^4(\omega_4^{(i)})^2 + \dots \quad (20)$$

$$j\eta_{\text{tot}}^{(i)} = \mu\eta_1^{(i)} + \mu^3\eta_3^{(i)} + \mu^5\eta_5^{(i)} + \dots \quad (21)$$

In the equations, under conditions of $\beta_{se} \leq 1$, $\beta_{ke} \leq 1$ and $\eta_{\max} \ll 1$, we can get $\eta_{\max}\beta_{se} \ll 1$ and $\eta_{\max}\beta_{ke} \ll 1$. Therefore, $\mu\beta_{se}$ and $\mu\beta_{ke}$ can be considered as small parameter like μ . In these equations, $\{\phi^{(i)}\}_0$, $\{\phi^{(i)}\}_1$, $\{\phi^{(i)}\}_2$, ... and $(\omega_0^{(i)})^2$, $(\omega_2^{(i)})^2$, $(\omega_4^{(i)})^2$, ... and $\eta_1^{(i)}$, $\eta_3^{(i)}$, $\eta_5^{(i)}$, ... have real quantities.

By substituting these equations from Eqs. (19) to (21) into Eq. (17), the following equation can be obtained:

$$\eta_{\text{tot}}^{(i)} = \eta_{se}^{(i)} - \eta_{ke}^{(i)} \quad (22)$$

$$\eta_{se}^{(i)} = \sum_{e=1}^{e_{max}} (\eta_e S_{se}^{(i)}) , S_{se}^{(i)} = \{\phi^{(i)}\}_0^T [K_R]_e \{\phi^{(i)}\}_0 / \sum_{e=1}^{e_{max}} \{\phi^{(i)}\}_0^T [K_R]_e \{\phi^{(i)}\}_0$$

$$\eta_{ke}^{(i)} = \sum_{e=1}^{e_{max}} (\chi_e S_{ke}^{(i)}) , S_{ke}^{(i)} = \{\phi^{(i)}\}_0^T [M_R]_e \{\phi^{(i)}\}_0 / \sum_{e=1}^{e_{max}} \{\phi^{(i)}\}_0^T [M_R]_e \{\phi^{(i)}\}_0$$

For the expressions, modal loss factor $\eta_{tot}^{(i)}$ can be computed using $\eta_{se}^{(i)}$ and $\eta_{ke}^{(i)}$. $\eta_{se}^{(i)}$ can be determined using share $S_{se}^{(i)}$ of strain energy of each element to total strain energy and material loss factors η_e of each element e . $\eta_{ke}^{(i)}$ can be determined using share $S_{ke}^{(i)}$ of kinetic energy of each element to total kinetic energy and material loss factors χ_e of each element e . While the material loss factors η_e are related hysteresis damping in the relation between stress and strain, the material loss factors χ_e are related flow resistance. The eigenmodes $\{\phi^{(i)}\}_0$ in Eqs. (22) has real quantity. Thus, the eigenmodes can be calculated by solving real eigenvalue problem, which corresponds to the equation by deleting all damping parameters in Eq. (17). We named the Eqn. (22) as Modal Strain and Kinetic Energy Method (MSKE method) [7]-[11]. This method corresponds to the extended version of Modal Strain Energy Method (MSE method) for structures including elastic bodies with viscoelastic bodies [17].

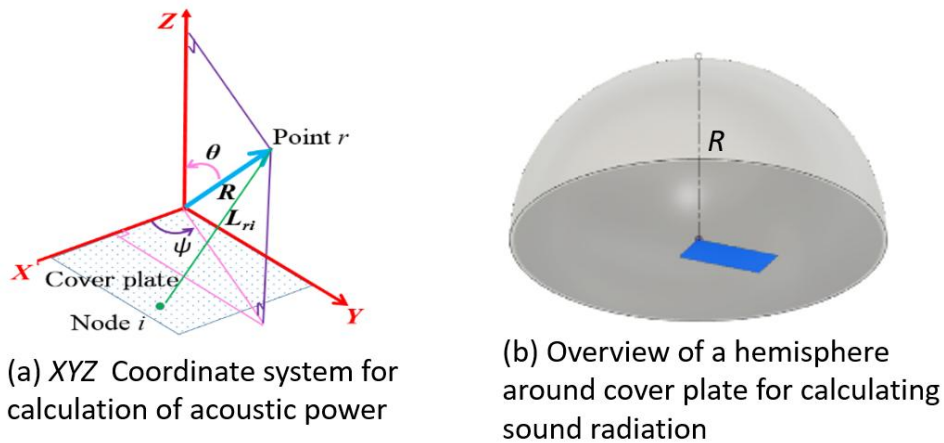


Fig. 5. Local coordinate and model for sound radiation from cover plate.

3.5 Computation of Vibration Responses and Acoustic Radiation Power Using MSKE Method [7]-[11]

Under input force, displacements $\{u_{out}\}$ as vibration responses in the structures are calculated using the modal parameters and modal damping from MSKE method in Sec.3.4 as follows.

$$\{u_{out}\} = \sum_{i=1}^{max} \frac{\{\phi_{in}^{(i)}\}^t \{F_{in}\} \{\phi_{out}^{(i)}\}}{m^{(i)} [(\omega^{(i)})^2 - \omega^2 + j(\omega^{(i)})^2 \eta_{se}^{(i)} - j\omega^2 \eta_{ke}^{(i)}]} \quad (23)$$

Where, $\{F_{in}\}$: external force vector at the excitation points, $\{\phi_{in}^{(i)}\}$: the i -th eigenmode at the excitation points, $\{\phi_{out}^{(i)}\}$: the i -th eigenmode at the observation points, $m^{(i)}$: the i -th modal mass.

Next, we consider sound radiation from the vibration in the cover plate to free sound field. Figure 5 shows a calculation model around the surface of the cover plate having local coordinate system XYZ for calculation of sound radiation. We set the origin at one of the corner in the cover plate. We introduce a hemisphere face like a dome having radius R around the cover plate. In this paper, we set R as 10m. The center of the hemisphere face is at the origin. There exists the cover plate at the bottom of the hemisphere. We evaluate the acoustic radiation power on the hemisphere face. We assume that there is an infinite baffle around the cover plate.

The sound pressure P_{ri} , radiated from the cover plate, can be expressed using Eq. (24) at a point r : $(X_r, Y_r, Z_r) = (R(\sin\theta)(\cos\phi), R(\sin\theta)(\sin\phi), R\cos\theta)$ on the hemisphere face.

$$P_{ri} = (j\omega u_{out,i})j\rho_0\omega A_i e^{-jk_0 L_{ri}} / 2\pi L_{ri} \quad (24)$$

Where, $v_{out,i} = j\omega u_{out,i}$ is the vibration velocity at the i -the node having the coordinate $(X_i, Y_i, 0)$. L_{ri} is the distance between the point r on the hemisphere face and the i -th node on the cover plate. A_i is the corresponding area relating the i -the node on the vibration surface of the cover plate. $k_0 = \omega/c_0$, ρ_0 and c_0 are the mass density and the sound speed of the air, respectively.

The sound pressure P_r at the point r can be calculated using the following equation considering the radiation from all nodes on the surface of the cover plate.

$$P_r = \sum_{i=1} (P_{ri}) \quad (25)$$

When the point r is sufficiently away from the surface of the cover plate, the acoustic intensity I_r can be expressed as $I_r = P_r^* P_r / (\rho_0 c_0)$. * stands for the complex conjugate. Thus, the acoustic radiation power W can be computed from the all surface of the cover plate as follows.

$$W = (1/2) \int_0^{2\pi} \int_0^{\pi/2} I_r R^2 (\sin\theta) d\theta d\phi \quad (26)$$

We evaluate effects of the acoustic black hole on sound radiation using Eq. (26).

4. Results and Discussion

4.1. Validity of Computation Method for a Flat Plate Having Krylov's Acoustic Black Hole.

Firstly, we try to compare between Krylov's experiment [5] and our numerical analysis of the flat panel with the acoustic black hole to check the validity of our calculation method and our code. The geometry of the panel in the Krylov's experiment is same with that of the cover plate in the double walls in this paper. For steel panel with the Krylov' type acoustic black hole, Young's modulus E is $E = 210\text{GPa}$. The mass density ρ is $\rho = 7.8\text{E}+03\text{kg/m}^3$. The material loss factor η is $\eta = 0.001$. The edge of the acoustic black hole has the same material properties with the steel panel. For boundary condition, all edges are free. For the flat region in the panel, the thickness is 5.04mm. In the edge of the panel with the black hole, the function of decreasing thickness $h(x)$ is $h(x) = \epsilon x^m$ ($m=2.2$), where x is distance from the edge. In Fig.6, the experimental results (Fig.6(a)) by Krylov [5] are compared with our calculated results (Fig.6(b)) by our group using our own original codes including 3D FEM and Modal Strain and Kinetic Energy Method. In these figures, the blue solid lines show results without damping layer on the black hole, and the red dotted lines represent those with damping layer on the black hole. Our computation can reproduce the black hole effects in the experiment.

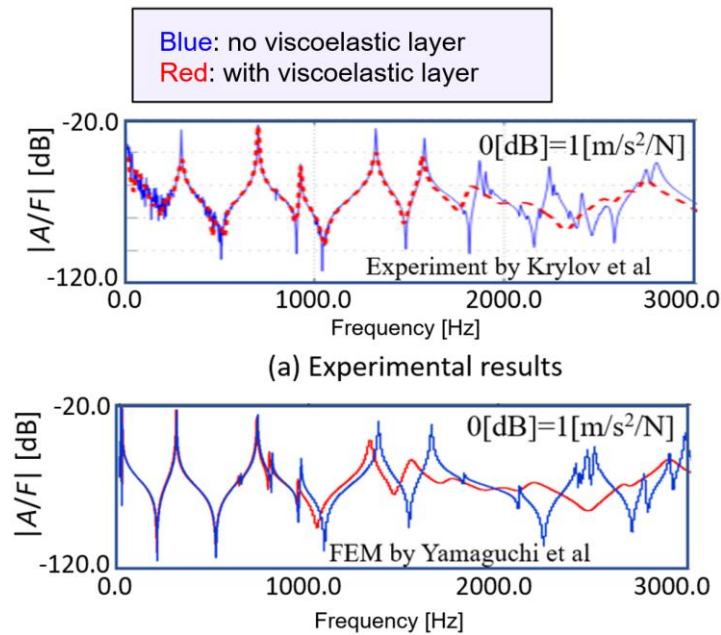


Fig. 6. Comparison of vibration responses for a flat plate having acoustic black hole between Krylov’s experiment [5] and our calculation using FEM with MSKE method.

4.2. Evaluation of Reduction in Sound Radiation due to Adding the Acoustic Black Hole

Figure 7 shows the acoustic radiation power from the cover plate with /without the acoustic black hole. In this figure, the ordinate stands for W/F_{in} (W : acoustic radiation power Watt, F_{in} : input N). The blue dotted line shows results without the acoustic black hole in the cover plate. As for the blue line, there are sharp peaks corresponding to the resonances of the double walls because of low damping. The red solid line represents results with the black hole. It can be seen that the acoustic radiation power for the cover plate with the black hole is much less than that for no black hole over all frequency region. Especially, in the higher frequency, very large reduction can be obtained. This phenomenon can be explained as follows.

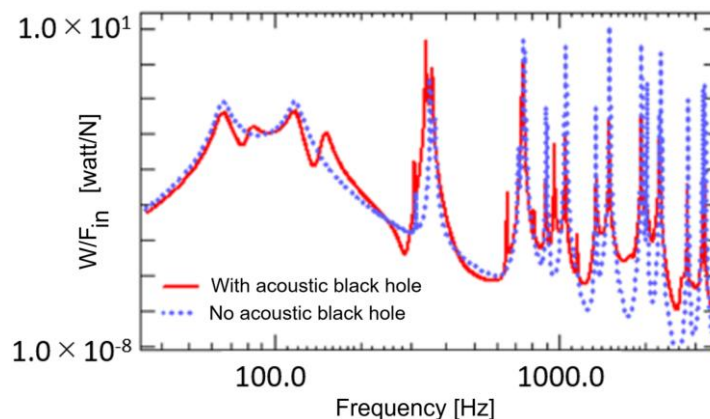


Fig. 7. Sound radiation with/without acoustic black hole.

The critical coincidence frequency of this steel cover plate (thickness: 5.04mm) is about 3000Hz. It is known that damping treatment is effective to reduce sound radiation in the higher frequency region than the critical coincidence frequency. On the other hand, the Krylov’s acoustic black hole has higher damping in the higher frequency region than 1600Hz. Therefore, large reduction in the sound radiation is notably observed in the high frequency region. Further, in the acoustic black hole, we experienced

that very short wave lengths are observed when the black hole yields high damping. Generally, if the wave length of the air is longer than the wave length of structural vibration, sound radiation can be reduced because cancelation occurs more easily among plus and minus amplitudes in each vibration mode when vibration is transferred to sound. In the region around the acoustic black hole, we can obtain extraordinary short wave lengths in the vibration (see Fig.8 as a typical example). This implies that sound radiation can be reduced due to short wave lengths in the vibration around the acoustic black holes in the cover plate.

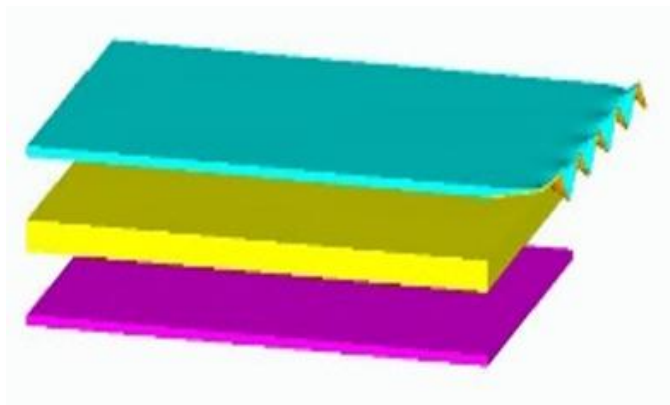


Fig. 8. An example of local deformation having short wave length at the edge of the cover plate with the acoustic black hole.

5. Conclusions

In this paper, we perform numerical analysis of damped vibration and sound radiation for structures having a porous layer sandwiched by double walls. The double walls are composed of a steel base plate and a steel cover plate. The cover plate in double walls has a Krylov type acoustic black hole at one edge of the plate. Viscoelastic damping material is laminated on the surface of the black hole. One point in the base plate is excited using white noise. Numerical analysis is performed to clarify changes of acoustic radiation from the cover plate due to the acoustic black hole using FEM and MSKE method (Modal Strain and Kinetic Energy method) proposed by Yamaguchi et al. Sound radiation from the cover plate decreased due to existence of the acoustic black hole in the cover plate. This is because of high damping due to the acoustic black hole. In the region around the acoustic black hole, we can obtain extraordinary short wave lengths in the vibration. This also causes that sound radiation can be decreased. This is because cancelations can more easily occur during radiation due to shorter wave lengths in the vibration around the acoustic black holes in the cover plate.

Acknowledgement

This research is supported by Suzuki Foundation Research Grant.

References

- [1] M.A. Mironov, "Propagation of a flexural wave in a plate whose thickness decreases smoothly to zero in a finite interval", *Soviet Physics-Acoustics*, Vol.34, pp.318–319, 1988.
- [2] V.V. Krylov, "Laminated plates of variable thickness as effective absorbers for flexural vibrations", *Proceedings of the 17th ICA* (Rome, Italy), September 2001.
- [3] V.V. Krylov, F.J.B.S. Tilman, "Acoustic 'black holes' for flexural waves as effective vibration dampers", *Journal of Sound and Vibration*, Vol.274(3–5), pp.605–619,2004.

- [4] V.V. Krylov, “New type of vibration dampers utilizing the effect of acoustic ‘black holes’ ”, *Acta Acustica united with Acustica*, Vol.90(5), pp.830–837, 2004.
- [5] V.V. Krylov, V. Kralovic, D.J. O’Boy, “Damping of flexural vibrations in rectangular plates using the acoustic black hole effect”, *Journal of Sound and Vibration*, Vol.329, pp.4672-4688,2010.
- [6] H.Oberst, *Akustische Beihefte* , Vol.4, pp.181-194,1952.
- [7] T. Yamaguchi, Y. Kurosawa and S. Matsumura, “FEA for damping of structures having elastic bodies, viscoelastic bodies, porous media and gas”, *Mechanical Systems and Signal Processing*, Vol.21(1), pp.535-552, 2007.
- [8] T. Yamaguchi, I. Shirota, H. Enomoto and Y. Kurosawa, “Vibration transmission between double walls in cars with damping and sound bridges”, *Noise Control Engineering Journal*, Vol.58(3), pp.273-282, 2010.
- [9] T. Yamaguchi, Y. Kurosawa and H. Enomoto, “Damped vibration analysis using finite element method with approximated modal damping for automotive double walls with a porous material”, *Journal of Sound and Vibration*, Vol.325, pp.436-450, 2009.
- [10] K. Takebayashi, A. Tanaka, K. Andow and T. Yamaguchi, “Modal loss factor approximation for u-p formulation FEM using modal strain and kinetic energy method”, *Journal of Sound and Vibration*, Vol.505, pp.1–14, 2021.
- [11] T. Yamaguchi, H. Hozumi, Y. Hirano, K. Tobita and Y. Kurosawa, “Nonlinear transient response analysis for double walls with a porous material supported by nonlinear springs using FEM and MSKE method”, *Mechanical Systems and Signal Processing*, Vol.42, pp.115-128, 2014.
- [12] H. Utsuno, T. W. Wu, A. F. Seybert and T. Tanaka, “Prediction of sound fields in cavities with sound absorbing materials”, *AIAA Journal*, Vol.28 (11), pp.1870-1875, 1990.
- [13] Y. J. Kang and S. Bolton, “Finite element modeling of isotropic elastic porous materials coupled with acoustical finite elements”, *Journal of the Acoustical Society of America*, Vol.98(1), pp.635-643, 1995.
- [14] N. Attala, R. Panneton, and P. Debergue, “A mixed pressure-displacement formulation for proelastic materials”, *Journal of the Acoustical Society of America*, Vol.104 (3), pp.1444-1452, 1998.
- [15] M. A. Biot, Theory of propagation of elastic waves in a fluid-saturated porous solid”, *Journal of the Acoustical Society of America*, Vol.28 (2), pp.168-178, 1955.
- [16] B. A. Ma, and J. F. He, “A finite element analysis of viscoelastically damped sandwich plates”, *Journal of Sound and Vibration*, Vol.152(1), pp.107-123, 1992.
- [17] C. D. Johnson and D. A. Kienholz, “Finite element prediction of damping structures with constrained viscoelastic layers”, *AIAA Journal*, Vol.20(9), pp.1284-1290, 1982.
- [18] A. Pelata, F. Gautiera, S. C. Conlonb, F. Semperlottic “The acoustic black hole: A review of theory and applications”, *Journal of Sound and Vibration*, Vol.476, pp.1–24, 2020.